

To appear in ApJ

On the tidal interaction of a solar-type star with an orbiting companion: Excitation of g mode oscillation and orbital evolution

C. Terquem^{1,3}, J.C.B. Papaloizou², R.P. Nelson² and D.N.C. Lin¹

ABSTRACT

We calculate the dynamical tides raised on a non-rotating solar-type star by a close stellar or planetary companion. Dissipation arising from a turbulent viscosity operating in the convection zone and radiative damping in the radiative core are considered.

We compute the torque exerted on the star by a companion in circular orbit, and determine the potentially observable magnitude of the tidally induced velocity at the stellar photosphere. These calculations are compared with the results obtained by assuming that a very small frequency limit can be taken in order to calculate the tidal response (*equilibrium tide*). For a standard solar model, the latter is found to give a relatively poor approximation at the periods of interest of several days, even when the system is far from resonance with a normal mode. This behavior is due to the small value of the Brunt-Väisälä frequency in the interior regions of the convection zone.

It is shown that although the companion may go through a succession of resonances as it spirals in under the action of the tides, for a fixed spectrum of normal modes its migration is controlled essentially by the non-resonant interaction.

We find that the turbulent viscosity that is required to provide the observed circularization rates of main sequence solar-type binaries is about fifty times larger than that simply estimated from mixing length theory for non-rotating stars. We discuss the means by which this enhanced viscosity might be realized.

These calculations are applied to 51 Pegasi. We show that the perturbed velocity induced by the tides at the stellar surface is too small to be observed. This result is insensitive to the magnitude of the turbulent viscosity assumed and is not affected by the possibility of resonance. For this system, the stellar rotation and the orbital motion are expected to be synchronized if the mass of the companion is as much as one tenth of a solar mass.

¹UCO/Lick Observatory, University of California, Santa-Cruz, CA 95064, USA – ct, lin@ucolick.org

²Astronomy Unit, School of Mathematical Sciences, Queen Mary & Westfield College, University of London, Mile End Road, London E1 4NS, UK – J.C.B.Papaloizou, R.P.Nelson@qmw.ac.uk

³*On leave from:* Laboratoire d’Astrophysique, Observatoire de Grenoble, Université Joseph-Fourier/CNRS, BP 53, 38041 Grenoble Cedex 9, France

Subject headings: hydrodynamics — waves — binaries: close — stars: late-type — stars: oscillations — planets and satellites: general

1. Introduction

Theoretical analyses of the tidal interaction between close binaries can be classified according to whether an equilibrium tide is assumed or the dynamical tide is taken into account. The theory of the equilibrium tide is based on the assumption that a star subject to the tidal disturbance of a companion instantly adjusts to hydrostatic equilibrium (Darwin 1879). A calculation including the dynamical tide takes into account the fact that gravity or g modes can be excited in the convectively stable layers of the star and that resonances between the tidal disturbance and the normal modes of the star can occur (Cowling 1941). So far, dynamical tides have been studied only in massive close binaries, which have a convective core and a radiative envelope (Zahn 1975, 1977; Savonije & Papaloizou 1983, 1984, 1997; Papaloizou & Savonije 1985, 1997; Savonije, Papaloizou & Alberts 1995).

In this paper, we examine the effect of dynamical tides excited by a companion on a solar-type star, in which a radiative core is surrounded by a convective envelope.

This is of particular interest in connection with circularization of solar-type binaries. It has been proposed that circularization occurs through the action of turbulent viscosity, originating in the convective envelope, on the tide. However, according to Claret & Cunha (1997) (see also Goodman & Oh 1997), who have used the equilibrium tide formalism of Zahn (1989), the circularization rate resulting from this mechanism is too small by about two orders of magnitude to account for the circularization timescales required on the main sequence.

The tidal response calculation undertaken here is also of interest in connection with the newly discovered planets, some of which are found to orbit around solar-type stars with a period comparable to that of the high order g modes of the star. One such example is 51 Pegasi (Mayor & Queloz 1995; Marcy & Butler 1995).

In these binaries, g mode oscillations are excited by the companion in the radiative region beneath the convective envelope. They become evanescent in the convection zone where they are damped by their interaction with the convective eddies. This dissipation leads to an exchange of angular momentum between the star and the orbit if the stellar rotation and the orbital motion are not synchronized. Here we assume that the orbital frequency is initially larger than the rotational frequency of the star. Then tidal interaction results in the decay of the orbit and the spin up of the star. If the mass of the secondary companion is considerably smaller than that of the primary, the timescale for orbital decay is smaller than the stellar spin up timescale, and the companion eventually plunges into the primary. But if the mass of the companion is large enough,

synchronization may occur before the binary has merged, stopping further orbital decay. Estimates based on the theory of the equilibrium tide (Rasio *et al.* 1996; Marcy *et al.* 1997) suggest that the orbital decay timescale and the stellar spin up timescale for a system like 51 Pegasi are longer than the inferred age of the primary if the companion is a Jovian like planet.

In this paper we examine the effect of resonances on these timescales, and determine the potentially observable magnitude of dynamical tides at the photosphere of a solar-type star. We also compare the dynamical tide calculations with the results of an asymptotic analysis we carry out in the limit of small frequencies which should correspond to the adiabatic equilibrium tide theory.

The paper is organized as follows: In §2, we study the tidal response of the star to the perturbation by a companion in a circular orbit with a period in the range 4–13 days. In § 2.1, we first consider the linear adiabatic response and then, away from resonance with a g mode, extend the analysis using first order perturbation theory to calculate the torque due to dissipation in the convective envelope. This mechanism is then found to be more important than non-adiabaticity arising from heat transport in the radiative interior (i.e. radiative damping). However, this is not the case in the vicinity of a g mode resonance. There we also calculate the torque due to non-adiabaticity in the radiative core using a WKB treatment of the non-adiabatic terms. We find that the torque at effective resonances is mainly determined by radiative damping. An analysis valid for very low frequencies (*equilibrium tide*) is given in § 2.2.

The orbital circularization timescale for systems initially in non-circular orbits can be derived from the response calculations for companions in circular orbits. This is done in § 2.3. We then discuss how this might be used to calibrate the magnitude of the turbulent viscosity required to fit the observations in § 2.4.

Numerical calculations are presented in §3. The results assuming the equilibrium tide are given in § 3.1. In § 3.2 we present the results of the dynamical tide calculations. We describe the tidal response of the star to a companion in circular orbit, give the induced velocity at its surface and the tidal torque. We describe the resonances and show that, for the periods of interest of several days, they are not expected to affect the orbital evolution of the binary. In § 3.3 we compare the calculations based on the dynamical and equilibrium tides. We find that, for the standard solar model, at the orbital periods of interest, because of the long timescale associated with convection, the equilibrium tide calculations give a relatively poor approximation to the results of the dynamical tide calculations.

We find that the viscosity that is required to provide the observed circularization rates is about 50 times larger than that simply estimated from mixing length theory and discuss the means by which this viscosity might be enhanced in § 3.4. However, we note that *the strength of the resonances for orbital periods larger than ~ 8 days and the perturbed velocity at the surface of the star are insensitive to the magnitude of the turbulent viscosity assumed*. Only for periods ~ 4 days is the strength of the resonances decreased by a factor ~ 4 . The observable width of the

resonances as well is reduced when the viscosity is increased. We also give the relation between the orbital evolution, circularization and spin up timescales and the orbital frequency in § 3.5.

Finally in §4 we discuss and summarize our results, applying them to 51 Pegasi in §4.1.

2. Tidal response to a companion in circular orbit

The calculations presented in this section will be applied to close binary systems where the primary is a solar-type star and the secondary a stellar or planetary companion. The orbital periods of interest lie in the range 4–13 days. The rotational angular velocity of the primary is assumed to be small compared to the orbital frequency, so that it can be neglected. Quadrupolar tidal forcing thus occurs through potential perturbations with periods in the range 2–6.5 days.

When calculating the tidal response well away from a condition of resonance with a g mode, we firstly calculate the tidal response assuming it to be adiabatic throughout the star. First-order perturbation theory is then used to calculate the dissipation occurring in the convective envelope. The idea here (as is borne out by the numerical results) is that although short wavelength g modes are excited in the radiative core, when they are away from resonance they do not play an important role in comparison to the global component of the tidal response. Also the variations in the convective envelope occur on a comparatively long length scale, making the adiabatic approximation a reasonable one.

When there is a resonance with a high order g mode, the response becomes one with a very short length scale such that non-adiabaticity in the radiative core cannot be neglected. However, the modes are of high order such that a WKB treatment of the non-adiabatic effects is possible and this is used close to resonance where the normal mode dominates the response. Such non-adiabatic effects turn out to be more important than the action of turbulent viscosity in the convective envelope, with the torque at significant resonances being determined mainly by non-adiabatic effects.

2.1. Linearized equations

2.1.1. Adiabatic perturbations

The linearized momentum, mass, and energy equations governing the adiabatic response of the non-rotating star to the perturbing potential Ψ_T may be written (see, for example, Unno *et al.* 1989)

$$\frac{\partial^2 \xi}{\partial t^2} = -\frac{1}{\rho} \nabla P' + \frac{\rho'}{\rho^2} \nabla P - \nabla \Psi_T, \quad (1)$$

$$\rho' = -\nabla \cdot (\rho \boldsymbol{\xi}), \quad (2)$$

$$\Delta S = 0, \quad (3)$$

where P is the pressure, ρ is the density, S is the entropy, $\boldsymbol{\xi}$ is the Lagrangian displacement vector, Δ denotes the Lagrangian perturbation and the primed quantities are Eulerian perturbations. We use the Cowling (1941) approximation, applicable to stars with high central condensation, which neglects the perturbation to the stellar gravitational potential. We also have the thermodynamic relation

$$\Delta S = \frac{P}{\rho T} \frac{1}{\Gamma_3 - 1} \left(\frac{\Delta P}{P} - \Gamma_1 \frac{\Delta \rho}{\rho} \right), \quad (4)$$

where T is the temperature and Γ_1 and Γ_3 are the adiabatic exponents of Chandrasekhar. This relation together with equation (3) leads to

$$\frac{\rho'}{\rho} = \frac{P'}{\Gamma_1 P} - A \xi_r, \quad (5)$$

where

$$A = \frac{d \ln \rho}{dr} - \frac{1}{\Gamma_1} \frac{d \ln P}{dr} = -\frac{N^2}{g}, \quad (6)$$

with $\text{sgn}(N^2) \times \sqrt{|N^2|}$ being the Brunt-Väisälä frequency and g the acceleration due to gravity.

Following Cowling (1941), only the dominant quadrupole term is considered in the perturbing potential due to the companion. For a binary system with a circular orbit, this is given in spherical polar coordinates (r, θ, φ) by the real part of

$$\Psi_T(r, \theta, \varphi, t) = f r^2 Y_{n,m}(\theta, \varphi) e^{-im\omega t}, \quad (7)$$

where the spherical harmonic

$$Y_{n,m}(\theta, \varphi) = P_n^{|m|}(\cos \theta) e^{im\varphi}$$

with $n = m = 2$, $P_n^{|m|}$ being the associated Legendre polynomial with indices n and m . Here ω is the orbital angular velocity, $f = -GM_p/4D^3$, where D is the orbital separation, and M_p is the mass of the companion. We adopt the same angular and time dependence for the perturbations, so that P' , ρ' and S' are proportional to $Y_{n,m}(\theta, \varphi) \exp(-im\omega t)$. The corresponding expression for the Lagrangian displacement is

$$\boldsymbol{\xi} = \left[\xi_r(r), \xi_h(r) \frac{\partial}{\partial \theta}, \xi_h(r) \frac{\partial}{\sin \theta \partial \varphi} \right] Y_{n,m}(\theta, \varphi) e^{-im\omega t}. \quad (8)$$

The factor $Y_{n,m}(\theta, \varphi) \exp(-im\omega t)$ will be henceforth taken as read, so that hereafter the perturbations will be taken to depend only on r . Physical perturbations are then found by taking real parts after inserting this factor.

The horizontal displacement ξ_h is given by the non-radial equation of motion (1):

$$\xi_h = \frac{1}{m^2 \omega^2 r} \left(\frac{P'}{\rho} + f r^2 \right). \quad (9)$$

This relation together with equation (5) allow P' and ρ' to be eliminated from the system (1)–(3). The radial equation of motion (1) and the continuity equation (2) can then be written as a pair of ordinary differential equations for ξ_r and ξ_h :

$$\frac{d\xi_r}{dr} = \left(-\frac{2}{r} + A - \frac{d \ln \rho}{dr} \right) \xi_r + \left[-\frac{m^2 \omega^2 r \rho}{\Gamma_1 P} + \frac{n(n+1)}{r} \right] \xi_h + \frac{f r^2 \rho}{\Gamma_1 P}, \quad (10)$$

$$\frac{d\xi_h}{dr} = \frac{1}{r} \left(1 - \frac{A P}{m^2 \omega^2 \rho} \frac{d \ln P}{dr} \right) \xi_r - \left(A + \frac{1}{r} \right) \xi_h + \frac{A f r}{m^2 \omega^2}, \quad (11)$$

the solution of which requires two boundary conditions. At the surface of the star we take a free boundary: $\Delta P = 0$, i.e. $P' = -\xi_r dP/dr$. The boundary condition at $r = 0$, where equations (10) and (11) have a regular singularity, is that the solutions be regular. Since at $r \sim 0$, $P = P_c + O(r^2)$, $\rho = \rho_c + O(r^2)$ and $A = O(r)$, where P_c and ρ_c are respectively the central pressure and density, this leads to $\xi_h = \xi_r/n$.

2.1.2. Torque due to dissipation in the convective envelope

The interaction between convective motions and the tidal flow is expected to lead to the dissipation of tidally excited waves (e.g. Zahn 1977). We model this effect as arising from a turbulent viscosity. To do this we suppose there is an additional dissipative force per unit mass acting in the convection zone given in spherical coordinates by:

$$\mathbf{F}_c = \frac{1}{\rho r^2} \frac{\partial}{\partial r} \left(\rho r^2 \nu \frac{\partial \mathbf{v}}{\partial r} \right), \quad (12)$$

where \mathbf{v} is the flow velocity and ν is the turbulent viscosity. Here, we assume that variation in the radial direction is the most significant and note that the viscous force is defined in such a way as to lead to a positive definite energy dissipation rate.

For the turbulent viscosity coefficient, we take (see, for example, Xiong, Cheng & Deng 1997)

$$\nu = \frac{c_1}{t_c} \frac{\Lambda^2}{1 + c_2 (mt_c/P_o)^s}, \quad (13)$$

where c_1 and c_2 are two constants, c_1 being on the order of unity, $P_o = 2\pi/\omega$ is the orbital period, Λ is the mixing length, and $t_c = 1/\sqrt{|\mathcal{N}^2|}$ is the convective timescale. The viscosity is then $c_1\Lambda^2/t_c$ for small forcing frequency $m\omega$. The factor $1 + (mt_c/P_o)^s$, where we shall use $s = 2$, allows for a reduction of efficiency of the damping of high frequency oscillations to which the convection cannot adjust. A similar prescription with $s = 1$ has been proposed by Zahn (1966) and used by Zahn (1989), whereas $s = 2$ has been considered by Goldreich & Keeley (1977) and used by Campbell & Papaloizou (1983) and Goldman & Mazeh (1991). Goodman & Oh (1997) have also recently put forward some arguments in favor of $s = 2$. For the mixing length, we shall take the standard relation $\Lambda = \alpha/|d\ln P/dr|$ and set $\alpha = 3$.

In principle, equations (1)–(3) should be solved with \mathbf{F}_c added on the right hand side of equation (1) in the convective envelope. However, this would increase the order of the differential system to be solved and make the numerical calculations much more complicated. Instead, we have found it adequate to solve first the adiabatic problem and then to treat the dissipative effect using a first-order perturbation theory. This is valid everywhere, except very close to resonances, because dissipation is weak enough so that the imaginary parts of ξ_r and ξ_h are much smaller in magnitude than their real parts. Thus we solve equations (1)–(3) without dissipative terms, and use these (real) solutions to calculate the rate of energy dissipation dE/dt due to convection which is given by:

$$\frac{dE}{dt} = - \int_{V_c} \rho \operatorname{Re}(\mathbf{F}_c) \cdot \operatorname{Re}(\mathbf{v}) \, dV, \quad (14)$$

where the integration is over the volume V_c of the convective envelope and the angular dependence of \mathbf{F}_c and \mathbf{v} has to be taken into account. Using the relation $\mathbf{v} = \partial\boldsymbol{\xi}/\partial t$ and the expression (8) for $\boldsymbol{\xi}$, we get

$$\frac{dE}{dt} = -\frac{48\pi}{5} m^2 \omega^2 \int_{R_i}^{R_c} \rho r^2 \nu \left[\left(\frac{\partial \xi_r}{\partial r} \right)^2 + 6 \left(\frac{\partial \xi_h}{\partial r} \right)^2 \right] dr, \quad (15)$$

where R_i and R_c are respectively the inner and outer radius of the convective envelope. Noting that the ratio of the rate of exchange of energy and angular momentum with the orbit is given by the pattern speed of the tidal disturbance, ω , the torque exerted by the companion on the star is given by

$$\mathcal{T} = -\frac{1}{\omega} \frac{dE}{dt}. \quad (16)$$

This torque is positive because the star is non-rotating.

When the frequency of the tidal wave is equal to that of some adiabatic normal mode frequency of the star, we can no longer use first-order perturbation theory because it would give an infinite torque. However, when the frequency ω is very close to a resonant frequency ω_0 , the torque will be given by an expression of the form

$$\mathcal{T} = \frac{\mathcal{A}}{m^2(\omega - \omega_0)^2 + \gamma^2}, \quad (17)$$

where \mathcal{A} is an amplitude and γ is the damping rate for the mode. First-order perturbation theory assumes dissipative effects are small in the response calculation. Therefore it is valid only for frequencies such that $m^2(\omega - \omega_0)^2 \gg \gamma^2$. However, the damping rate, if small, can be found from first-order perturbation theory applied, as described above, very close to resonance where the mode dominates the response. Then it is given by (see, for example, Goldstein 1980)

$$2\gamma = -\frac{1}{2E_K} \frac{dE}{dt} \quad (18)$$

very close to resonance, where E_K is the kinetic energy of the mode:

$$E_K = \frac{1}{2} \int_V \rho [Re(v)]^2 dV = \frac{24\pi}{5} m^2 \omega^2 \int_0^R \rho r^2 (\xi_r^2 + 6\xi_h^2) dr, \quad (19)$$

the integration being over the volume V of the star (in the first integral, the angular dependence of \mathbf{v} has to be taken into account). In (18), the total energy of the mode is $2E_K$ because at resonance there is equipartition between kinetic and potential energy. We calculate γ using (18) as outlined above making sure that ω is close enough to ω_0 by checking that γ remains approximately constant when ω is slightly changed. To get \mathcal{A} , we fit the torque obtained from first-order perturbation theory to the expression (17) in the region approaching the resonance where still $m^2(\omega - \omega_0)^2 \gg \gamma^2$. This procedure works satisfactorily when γ is small with consequent strong resonances. This appears to be the situation when turbulent viscosity alone is assumed to act. However, radiative damping cannot be neglected for resonances at low forcing frequency and this is discussed below.

2.1.3. Torque due to non-adiabaticity in the radiative core

Non-adiabatic effects become important when the radiative diffusion time across the length scale associated with the tidal response shortens to become comparable to the wave propagation time across the star. In principle, these effects should be taken into account both in the radiative core and above the convection zone. However, since g modes, which are excited in the radiative

core, are evanescent in the convective envelope, we do not expect non-adiabaticity to play an important role above the convection zone. To take into account non-adiabatic effects, equation (3) has to be modified in the radiative core to:

$$\rho T \frac{\partial(\Delta S)}{\partial t} = -\nabla \cdot \mathbf{F}', \quad (20)$$

where \mathbf{F}' is the perturbed radiative flux. The radiative flux is given by the radiative diffusion equation

$$\mathbf{F} = -K \nabla T,$$

where T is the temperature and $K = 4acT^3/(3\kappa\rho)$ is the radiative conductivity, with a being the Stefan–Boltzmann radiation constant, c the velocity of light and κ the opacity. Therefore

$$\nabla \cdot \mathbf{F}' = -\frac{1}{r^2} \frac{\partial}{\partial r} \left[r^2 \left(K \frac{\partial T'}{\partial r} + K' \frac{dT}{dr} \right) \right] - \nabla_h^2 (KT'), \quad (21)$$

where ∇_h is the non-radial component of the operator ∇ . We now suppose that close to resonance, the response behaves exactly like a free g mode with very large radial wavenumber k_r so that WKB theory can be used together with the local dispersion relation to evaluate $\nabla \cdot \mathbf{F}'$. The dominant term in the right-hand side of (21) is then $-K\partial^2T'/\partial r^2 = Kk_r^2T'$, and all the other terms can be neglected. For a high order free g mode, the local dispersion relation gives (see, for example, Unno *et al.* 1989):

$$k_r^2 = \frac{N^2}{(m\omega)^2} \frac{l(l+1)}{r^2}. \quad (22)$$

This expression of k_r is derived under the adiabatic approximation. However, since we want to incorporate non-adiabatic effects to the lowest order, we do not need to take them into account in evaluating k_r . We have $k_r \gg 1/r$ in the radiative core because $N \gg m\omega$ there. The perturbed temperature T' can be expressed as a function of P' and ρ' using the thermodynamic relation

$$\frac{T'}{T} = \frac{1}{\chi_T} \frac{P'}{P} - \frac{\chi_\rho}{\chi_T} \frac{\rho'}{\rho}, \quad (23)$$

where $\chi_T = \partial \ln P / \partial \ln T)_\rho$ and $\chi_\rho = \partial \ln P / \partial \ln \rho)_T$.

The equation of state in the radiative core of a solar-type star is primarily that of a perfect gas (we neglect here the radiation pressure which is very small compared to the gas pressure). We then have $\Gamma_1 = \Gamma_3 = 5/3$ and $\chi_\rho = \chi_T = 1$. Using the above, the fact that $l = 2$, $\partial/\partial t = -im\omega$ and the relation (4), we can recast (20) under the form

$$\frac{\rho'}{\rho} = \frac{1+i\epsilon\Gamma_1}{1+i\epsilon} \frac{P'}{\Gamma_1 P} - \frac{A}{1+i\epsilon} \xi_r, \quad (24)$$

where

$$\epsilon = \frac{16acT^4N^2}{5(m\omega)^3\kappa\rho P r^2}. \quad (25)$$

For high order free g modes, we have (see, for example, Unno *et al.* 1989)

$$\frac{P'/P}{A\xi_r} \sim \frac{m\omega}{N} \frac{d\ln P}{d\ln r},$$

which means that $P'/P \ll A\xi_r$ in the radiative core of a solar-type star at the frequencies of interest. The non-adiabatic correction of the term associated with pressure in equation (24) is then very small compared to the non-adiabatic correction of the term involving ξ_r . Therefore equation (24) can be approximated by

$$\frac{\rho'}{\rho} = \frac{P'}{\Gamma_1 P} - \bar{A}\xi_r, \quad (26)$$

where we have defined $\bar{A} = A/(1+i\epsilon)$. We note that because we have identified the tidal response with a normal mode, this calculation is valid only close to resonances. Equation (26) is similar to (5) but with A being replaced by \bar{A} . The system of differential equations we have to solve to get the non-adiabatic response of the star is then the same as (10)–(11) but with the following modification in the radiative core. In equations (10) and (11), A , where it appears as a coefficient of ξ_r , has to be replaced by \bar{A} . The system of differential equations so obtained is complex. In general, for the periods we consider, $\epsilon \leq 5 \times 10^{-4}$ is small. We then calculate both the real and imaginary parts of the response, so that the torque can be computed directly from:

$$\mathcal{T} = - \int_V \rho' \frac{\partial \Psi_T}{\partial \varphi} dV \quad (27)$$

where the integral is over the volume V of the star. The angular dependence of Ψ_T and ρ' has to be taken into account in this expression. Equation (27) can be recast under the form (Savonije & Papaloizou 1983):

$$\mathcal{T} = -\frac{96\pi f}{5} \int_0^{R_\odot} \text{Im}(\rho') r^4 dr. \quad (28)$$

As in § 2.1.2, we can calculate the damping rate γ' in resonances due to non-adiabatic effects using (18). Here, the rate of energy dissipation is calculated from the torque (see 16).

2.2. Low frequency limit

In the limit of small $|\omega|$, the following relations may be obtained for the *adiabatic equilibrium tide*:

$$P'_{eq} = -fr^2\rho, \quad (29)$$

and, if $N^2 \neq 0$:

$$\xi_{r,eq} = fr^2\rho \left(\frac{dP}{dr} \right)^{-1}, \quad (30)$$

$$\xi_{h,eq} = \frac{1}{n(n+1)r} \frac{d}{dr}(r^2\xi_{r,eq}), \quad (31)$$

where the ‘*eq*’ subscript denotes the equilibrium value. Using these displacements, the torque may be calculated using equations (15) and (16).

However, we comment that equation (30), which states that the Lagrangian perturbation to the pressure is zero, can only be derived in the adiabatic low $|\omega|$ limit if the Brunt-Väisälä frequency is not zero (in practice, one also requires that the forcing period be short compared to the thermal timescale of the star, but the latter is so long that it can be assumed to be infinite in this context). Equations (30)–(31) do not apply in a finite region where strictly $N^2 = 0$. In that case the fluid is locally barotropic, and the displacement can be written as the gradient of a potential:

$$\boldsymbol{\xi} = \nabla [\Phi(r)Y_{n,m}]. \quad (32)$$

The continuity equation then gives for low frequencies

$$\nabla \cdot (\rho \boldsymbol{\xi}) = \frac{1}{r^2} \frac{d}{dr} \left(r^2 \rho \frac{d\Phi}{dr} \right) - \frac{n(n+1)\rho\Phi}{r^2} = -\rho'_{eq} = -\frac{P'_{eq}\rho}{\Gamma_1 P} = \frac{fr^2\rho^2}{\Gamma_1 P}. \quad (33)$$

Equation (33) gives a second order differential equation for $\Phi(r)$. This applies inside the region where $N^2 = 0$. It is possible, using the two available boundary conditions for (33), to match $\xi_{r,eq}$ given by (30) at the boundaries of such a region, but not in general $\xi_{h,eq}$ given by (31). This means that there will tend to be a discontinuity in the tangential displacement at the boundaries for low frequencies.

When $|N^2|$ is not zero but very small, in particular small compared to $m^2\omega^2$, which corresponds physically to the convective timescale being much longer than the forcing period, the tidal response more closely matches that given by (33) than that given by equations (30)–(31). This feature causes a very slow convergence towards the low frequency limiting solution (*equilibrium tide*)

found here, as well as near discontinuous behavior near the inner convective envelope boundary. This is borne out by our numerical results (see § 3.2.1 and § 3.3).

2.3. Timescales

2.3.1. Orbital evolution and stellar spin up timescales

The torque, \mathcal{T} , gives the rate at which angular momentum is transferred from the orbit to the star. We can then calculate a tidal evolution (decay) timescale of the circular orbit:

$$t_{orb} = \frac{\mu\omega D^2}{\mathcal{T}}, \quad (34)$$

where $\mu = M_p M_\odot / (M_p + M_\odot)$ is the reduced mass. In principle, the variation of the torque with ω has to be taken into account for the total decay time to be calculated. However, since the torque increases as the companion spirals in, t_{orb} is mainly determined by the initial position of the companion, and a good estimate can be obtained using the above formula.

This exchange of angular momentum also results in the spin up of the star, the timescale of which is given by $t_{sp} = I\omega/\mathcal{T}$ (Savonije & Papaloizou 1983), with I being the stellar moment of inertia. Out of resonance, angular momentum deposition *initially* occurs mainly in the convective envelope where the turbulent viscosity acts (Goldreich & Nicholson 1989). It is then of interest to calculate the spin up timescale for the convective envelope alone, which is $t_{sp,c} = I_c\omega/\mathcal{T}$, where I_c is the moment of inertia of the convection zone. We note however that on the long timescales associated with tidal evolution, angular momentum may be redistributed throughout the star.

2.3.2. Circularization

In practice, we find that the torque arising from a companion in a circular orbit varies with frequency approximately $\propto \omega^4$. This result can be used to relate the orbital circularization timescale to the initial orbital decay timescale provided that the eccentricity is not too large. In practice, both these timescales can be significantly longer than the spin up timescale of the star due to its relatively small moment of inertia. We should then consider that the star is synchronized with the orbit.

The ratio between the orbital decay timescale and the circularization timescale t_{circ} is found to be about 6 for the calculated frequency dependence of the circular orbit torque (see, for example, the expressions given in Savonije & Papaloizou 1983, 1984). This appears to be independent of whether the star is assumed to be synchronously rotating or non-rotating in that the circularization rate calculated assuming no rotation, as we do here, gives a reasonable estimate

in the synchronous case also. In addition, to evaluate t_{circ} for an equal mass system, we have to take into account the reciprocal torque exerted by the primary on the companion. To do this, we take t_{circ} to be proportional to a factor which is 1/2 when $M_p = M_\odot$ and 1 when $M_p \ll M_\odot$. To a reasonable approximation, we then get:

$$t_{circ} = \frac{t_{orb}}{6(1 + M_p/M_\odot)}. \quad (35)$$

2.4. Circularization timescale as a calibration of turbulent viscosity

One of the purposes of this paper is to calculate the tidally induced velocities on the star. In order to do this, the processes responsible for dissipating the disturbance should be included as accurately as possible. An important dissipation process is that associated with turbulent friction in the convection zone. As this process has been suggested as being responsible for circularizing the orbits of main sequence binaries of sufficiently short period (see Mathieu 1994), we investigate whether reasonable assumptions about the behavior of turbulent viscosity can lead to the observed circularization rates.

2.4.1. Background

Zahn & Bouchet (1989) have investigated the pre–main sequence evolution of late–type binaries in which the stars are fully convective. The main conclusion of their work was that circularization occurs at the very beginning of the Hayashi phase, with hardly any decrease of the eccentricity on the main sequence. The cutoff period they predict is between 7.3 and 8.5 days. According to them, observations show a cutoff period around 8 days independent on the age of the star and are then in agreement with their results.

However, we note that for this agreement to be reached, some observations had to be discarded. Those by Mayor & Mermilliod (1984), which indicated that the cutoff period of late–type binaries was at most 5.7 days, and those by Mathieu & Mazeh (1988), which showed that the cutoff period in the 4 *Gyr* old cluster M 67 was more than 10 days. In a review article, Mathieu (1994) (see also Mathieu 1992 and Mathieu *et al.* 1992) has confirmed that “cutoff periods increase with age, consistent with active main sequence tidal circularization”. The pre–main sequence cutoff period is very likely to be 4.3 *d* (an upper limit being 6.4 *d*), and cutoff periods for solar–mass binaries are 7.05 *d* in the Pleiades (0.1 *Gyr*), 8.5 *d* in the Hyades (0.8 *Gyr*), 12.4 *d* in M 67 (4 *Gyr*) and 18.7 *d* in the halo field (16 *Gyr*). We therefore conclude that active circularization does take place for main sequence binaries and that it is less efficient than proposed by Zahn & Bouchet (1989) on the pre–main sequence.

Recently, Claret & Cunha (1997) have applied the formalism developed by Zahn (1989) to

different stellar models. They have computed the parameters which enter into the expression for the circularization timescale, which is based on treatment of the equilibrium tide, for a wide grid of stellar models as a function of mass and time. Their conclusion is that turbulent dissipation is too low by a factor 100–200 during the main sequence to fit the observed cutoff periods.

3. Numerical results

The calculations presented in the following section are applied to the standard solar model described by Christensen–Dalsgaard *et al.* (1996).

3.1. Equilibrium tide

The torque associated with the equilibrium tide was calculated as indicated in § 2.2. As mentioned there, this calculation is only expected to apply at very low frequencies. For periods between 4.23 and 12.4 d , and $c_1 = c_2 = 1$, the calculated torque can be interpolated by the following power law:

$$\mathcal{T} \left(g.cm^2/s^2 \right) = 1.200 \times 10^{55} \left(\frac{M_p}{M_p + M_\odot} \right)^2 \omega^{4.08}. \quad (36)$$

3.2. Dynamical tide

For the calculation of the dynamical tide, we solve numerically the differential equations (10) and (11) using a shooting method to an intermediate fitting point (Press *et al.* 1986). To evaluate non-adiabatic effects in the radiative core close to resonances, we modify these equations in the way described in § 2.1.3. We define the dimensionless quantity $x \equiv r/R_c$, where R_c is the outer radius of the convective envelope. With this notation, the equations are integrated from $x_{in} = 10^{-6}$ to $x_{out} = 1.00071256$. The radiative core extends from $x = 0$ to $x \simeq 0.7$. The results presented below have been obtained with the values $c_1 = c_2 = 1$ and $\alpha = 3$ (α being the ratio of the mixing length Λ to the pressure scale height). We discuss the effect of changing these parameters.

3.2.1. Tidal response and velocity at the surface of the star

For illustration purposes, we plot the horizontal and radial displacements induced in the star at orbital periods of $P_o = 4.23 d$ and $8.46 d$ away from resonance in the adiabatic approximation. The first period is that inferred for the system 51 Pegasi. The spatial distribution of the real

parts of $m\omega\xi_r$ and $m\omega\xi_h$ are shown in Figure 1. These represent typical values of the radial and horizontal velocities, the maximum values being three and six times larger respectively. Since these quantities depend on the perturbing mass through the ratio $M_p/(M_p + M_\odot)$, they have been represented in units of this factor.

As expected, the stellar response shows oscillations between turning points near the center and the inner radius of the convection zone, where $m^2\omega^2 = N^2$, otherwise it is evanescent. The horizontal displacement varies rapidly in the photosphere because the temperature drops to zero rapidly there.

We see from Figure 1 that, when the perturbing mass $M_p = M_\odot$, the maximum radial velocity at the surface of the star is about 6 and 1 m/s for $P_o = 4.23$ d and 8.46 d respectively. These numbers drop to 10^{-2} and 2×10^{-3} respectively when the perturbing mass is one Jupiter mass ($M_p = 10^{-3}M_\odot$).

The radial displacement and the perturbed pressure at the surface of the star are well approximated by the equilibrium values (30) and (29) respectively. These quantities are found to be insensitive to the existence of resonances with the consequence that the radial velocity at the surface of the star never differs much from the values given above. For the smallest periods considered, the ratio $|Re(\xi_h)/Re(\xi_r)|$ at the surface of the star can vary by up to one order of magnitude on passage through resonance. This is due to the fact that ξ_h is proportional to $(P' - P'_{eq})/P$ (see 9). Even though this ratio remains small, it can vary by up to an order of magnitude as a resonance is passed through.

The numerical results indicate that both the amplitude and the wavelength of the response increase with the orbital frequency, in agreement with the theoretical expectation of a smaller radial order for higher frequencies (Christensen–Dalsgaard & Berthomieu 1991 and references therein).

Finally, as expected (see § 2.2), the plots shown in Figure 1 (see also Figure 3) indicate that at the boundary of the radiative core and the convection zone there is a near discontinuity in the mean value of ξ_h obtained after averaging out the interior oscillations.

3.2.2. Circular orbit torque

i) Resonances:

Figure 2 shows \mathcal{T} versus ω in a log–log representation for three different small frequency intervals in the vicinity of $P_o = 4.23$, 8.5 and 12.4 d. On each plot, the dotted line gives the values obtained from the theory of the equilibrium tide as given by (36). Since the torque depends on the perturbing mass through the factor $M_p^2/(M_p + M_\odot)^2$, it has been represented in units of this. These plots show several resonances, which occur when the frequency of the tidal wave is equal to the frequency of some normal mode of the star. The left panels show the torque arising from

convective dissipation, through turbulent viscosity, alone (see § 2.1.2). These plots have been displayed for comparison with the right panels, for which radiative damping has been taken into account in the resonances (see § 2.1.3).

As indicated by the Table 1, the normal mode damping rate due to radiative damping (γ') is much larger than that due to convective dissipation (γ).

Table 1: Normal mode damping rates

P_o (days)	ω (s^{-1})	γ (s^{-1})	γ' (s^{-1})
4.23	1.72×10^{-5}	6×10^{-12}	10^{-10}
8.5	8.56×10^{-6}	5×10^{-12}	7×10^{-10}
12.4	5.86×10^{-6}	4×10^{-12}	2×10^{-9}

Thus the torque in the center of resonances, where they are significant, is predominantly determined by radiative damping. For the frequencies we consider, this contribution to the torque becomes much smaller than that due to turbulent viscosity in the tail of the resonances. This means that non-adiabatic effects in the radiative core are negligible away from resonances. Therefore, in the right panels of Figure 2, we have plotted the torque resulting from radiative damping acting alone in the center of resonances, and that resulting from convective dissipation acting alone away from resonances. A comparison between the strength of the resonances shown in the right and left panels indicates the importance of non-adiabatic effects in the radiative core. As expected, the resonances are weakened and broadened, this effect being marginally important for $P_o \sim 4.23$ d.

We now discuss the properties and the effect of resonances on the tidal torque. From now on, when resonances are discussed, we shall refer to the calculations which take into account radiative damping.

In the neighborhood of $P_o = 4.23, 8.5$ and 12.4 d, the relative separation, $\Delta\omega/\omega$, between successive resonances is respectively 4.5×10^{-3} , 2×10^{-3} and 10^{-3} . The relative width, $\delta\omega/\omega$, of the resonances is respectively 3×10^{-4} , 1.5×10^{-4} and 10^{-4} . Here we have arbitrarily defined the width of a resonance as being the frequency interval over which \mathcal{T} is at least 3 times larger than the minimum torque obtained just out of this resonance.

To calculate the probability of the companion being in a resonance, we have to take into account the fact that it drifts away from the resonances much more rapidly than elsewhere. The relevant quantity for calculating the tidal evolution timescale is $1/\mathcal{T}$ (see expression 34). For a fixed oscillation spectrum, we can approximate this probability by $\delta\omega/\Delta\omega$ times the ratio of the mean value of $1/\mathcal{T}$ over a resonance to the mean value of $1/\mathcal{T}$ between two resonances, where the mean value is defined by

$$\left\langle \frac{1}{\mathcal{T}} \right\rangle = \int \frac{d\omega}{\mathcal{T}} / \int d\omega ,$$

with the integrals being taken over the relevant frequency interval.

This gives a probability of being in a resonance which is close to 0.7% for $P_o = 4.23$ and 8.5 d and 2% for $P_o = 12.4$ d . The fact that the probability of being in a resonance increases with P_o is not significant, because resonances get weaker when the period increases (see Figure 2).

We note that this discussion applies only if the *a priori* probability of being in any frequency interval of a given width is independent of the frequency as might be expected to be a reasonable assumption if the normal mode spectrum is fixed. However, different circumstances may apply if the combined effect of orbital and stellar evolution were to lock the companion in a resonance with changing location. But we shall not consider the possibility of this process here.

As the companion spirals inwards, it goes through a succession of resonances. However, for a fixed normal mode spectrum, the above calculation tells us that its migration is controlled essentially by the non-resonant interaction. This can be seen by comparing $\langle 1/\mathcal{T} \rangle$ evaluated over a large frequency range, both taking into account and neglecting the resonances. Such a comparison shows that neglecting resonances changes $\langle 1/\mathcal{T} \rangle$ by at most a few per cent.

ii) Relation between the mean torque, ω and the circularization timescale:

Here we interpolate the numerical results to express the torque as a power of the frequency. To begin with, we consider the three frequency intervals described above. We take the appropriate torque to be $1/\langle 1/\mathcal{T} \rangle$ where the mean values are taken over the frequency intervals displayed in Figure 2. The results can be interpolated with the following relation:

$$\mathcal{T} \left(g.cm^2/s^2 \right) = 1.654 \times 10^{53} \left(\frac{M_p}{M_p + M_\odot} \right)^2 \omega^{3.85}. \quad (37)$$

We have checked that the above formula gives a good estimate of the torque at other non-resonant frequencies between 4.23 and 12.4 d .

Since the index of the power law (37) is close to 4, the circularization timescale t_{circ} is given by (35). At $P_o = 12.4$ d , t_{circ} is found from the above formula to be 56 times larger than the timescale of 4 *Gyr* that is indicated by the observations.

We note that both the dynamical and equilibrium tide calculations give a power law with an index close to 4, which results in the circularization timescale being proportional to the binary period P_o to the $13/3$. For comparison, Zahn (1977), Zahn (1989) and Goldman & Mazeh (1991), using equilibrium tide calculations, found t_{circ} to be proportional to P_o raised to the power $16/3$, $13/3$ and $10/3$ respectively. The difference between these results can be related to a different choice of

s in the expression (13) for ν . These authors used an expression similar to (13) with respectively $s = 0, 1$ and 2 . The fact that we obtain an index close to $13/3$ by setting $s = 2$ or even $s = 1$ (see below), in contrast to the results above, is at least partially due to the effectively smaller value of c_2 we used (see below).

We comment further that Tassoul (1988) found $t_{circ} \propto P_o^{49/12}$ for his postulated alternative hydrodynamical mechanism for tidal circularization.

3.3. Comparison between calculations based on the dynamical and equilibrium tides

The results presented above show that the torque corresponding to the dynamical tide is smaller than that given by the adiabatic equilibrium tide for all the frequencies we have computed. However, the difference tends to decrease as the frequency gets smaller. From expressions (36) and (37), we calculate that the ratio of these torques is indeed about 6.0 and 4.8 for $P_o = 4.23$ and 12.4 d respectively.

Figure 3 shows $\xi_{r,eq}/R_c$, ξ_r/R_c and ξ_h/R_c in units $M_p/(M_p + M_\odot)$ versus x in the range $0.6 \leq x \leq x_{out}$ for $P_o = 4.23$ and 12.4 d .

It is clear from these plots that ξ_r departs from the asymptotic value in the convective envelope. The difference is not large, being about 17%, but the derivatives of ξ_r and ξ_h from which the torque is calculated (see 15) depart more from their asymptotic values.

In the limit where the magnitude of the Brunt-Väisälä frequency is everywhere large compared to the tidal forcing frequency, calculations based on the dynamical tide should converge towards those based on the equilibrium tide. This is because the convective timescale is small enough that the convective motions adjust essentially instantaneously to the tidal forcing.

We have checked this expectation by artificially increasing the magnitude of the Brunt-Väisälä frequency in the convection zone. Except in the part of the convective envelope just below its outer radius, wherever $|N^2| < q\omega^2$, q being an arbitrary constant, we make the replacement $N^2 = -q\omega^2$. In Figure 4 we plot $\xi_{r,eq}/\xi_r$ versus x in the range $0.6 \leq x \leq x_{out}$ for $P_o = 12.4$ d and for $q = 10, 100$ and 400 . For comparison we also plot the case corresponding to the original solar model.

As expected, $\xi_{r,eq}/\xi_r$ converges towards 1 when the magnitude of the Brunt-Väisälä frequency is increased. We note that $q = 400$, which corresponds to $|N| \geq 10m\omega$, gives $1 - \xi_{r,eq}/\xi_r$ smaller than 5%. This confirms that the asymptotic limit is reached when the magnitude of the Brunt-Väisälä frequency is very large compared to the frequency of the tidal wave.

We note that the very slow convergence towards the equilibrium tide was predicted from the arguments presented in § 2.2. Also expected was the discontinuity in the mean value of ξ_h , obtained after averaging out the interior oscillations, at the boundary of the radiative core and the convection zone that is observed in Figure 3 (see also Figure 1).

3.4. Calibration of the turbulent viscosity

We shall limit the comparison of our results with observations of main sequence binaries because our calculations do not apply to pre–main sequence stars, which have a much larger convective envelope than the Sun. As mentioned above, the observed circularization timescale we have to fit is then 4 *Gyr* for $P_o = 12.4$ *d* (Mathieu 1994). As indicated above, when using a simple estimate of the turbulent viscosity based on mixing length theory for non–rotating stars, the circularization timescale we get from our calculations for this period is 56 times larger than 4 *Gyr*. This indicates that either

- (i) solar–type binaries are not circularized through turbulent viscosity acting on tidal perturbations (but see Tassoul 1988 and Kumar & Goodman 1996 for other suggested tidal mechanisms), or
- (ii) dissipation in the convective envelope of solar–like stars is significantly more efficient than is currently estimated.

Tassoul (1995) postulates that efficient tidal dissipation occurs in a very thin Eckman layer close to the surface of a tidally deformed star and that this process greatly increases the efficiency of tidal interactions. But a refutation of the notion that the free surface boundary condition appropriate to the tidally deformed star, rather than the more common rigid boundary condition, leads to such an effective boundary layer, has been given by Rieutord & Zahn (1997). Further Tassoul & Tassoul (1997) state that their mechanism is inapplicable to extreme mass ratio cases such as 51 Pegasi that we consider later in the paper.

We now consider briefly here the mechanism proposed by Kumar & Goodman (1996), namely enhanced dissipation associated with high order oscillation modes excited through parametric instability. The growth rate for the most rapidly growing modes is expected to be $\sigma \sim m\omega\xi_r/R_\odot$, where ξ_r is the radial displacement in the primary oscillation, which we shall assume to be the equilibrium tide, evaluated at $r = R_\odot$, and $m\omega$ is its frequency.

If we assume that the non–linear development of the parametric instability and subsequent dissipation of the excited modes leads to an effective viscosity, and frictional dissipation rate $t_f^{-1} = \sigma$, which is big enough to suppress the linear instability, then we expect from the classical theory of Darwin (1879) that there will be a phase lag θ_t associated with the tide given by

$$\theta_t = \sigma \frac{R_\odot^3}{GM_\odot} \omega. \quad (38)$$

For a binary of unit mass ratio and period ~ 10 *d*, synchronization occurs on a timescale very much shorter than that required for circularization, so that we assume that the stellar rotation is synchronized with the orbit and $m = 1$ in the calculation of σ . For small eccentricity, the circularization timescale t_{circ} is approximately given by $1/t_{circ} = \Omega_a \theta_t$, where the apsidal motion frequency is $\Omega_a = 15k(M_p/M_\odot)(R_\odot/D)^5\omega$, with k being the apsidal motion constant (Cowling 1938). We use the equilibrium tide value (30) to estimate ξ_r/R_\odot at $r = R_\odot$ as

$(R_\odot/D)^3/4$ for a mass ratio of unity. We then get $1/t_{circ} = 7.5k\omega(R_\odot/D)^{11} \propto \omega^{25/3}$ for θ_t given by (38). For an orbital period of 12.4 d , this gives $t_{circ} = 6 \times 10^3/k\text{ Gyr}$. Since $k \sim 0.01$, it is not very likely that this mechanism will be able to explain the observed circularization rates. However, we stress that this has not been shown from a full non-linear calculation of the development of parametric instability.

3.4.1. Enhanced turbulent viscosity

In general, a large increase in the simply estimated turbulent viscosity coefficient is needed in order to explain the observed circularization rate. We now investigate what is needed to achieve this and give the numerical results of tests we have carried out. In all cases, we have checked that *the velocity at the surface of the star is not sensitive to the magnitude of the turbulent viscosity assumed*.

In addition, as indicated above, the resonances are essentially controlled by radiative damping in the radiative core as long as $\gamma' \gg \gamma$. When the turbulent viscosity is enhanced, γ is increased. However, in the tests we present below, for orbital periods larger than ~ 8 days, γ' stays large enough compared to γ so that, although the non resonant torques increase, the central structure and strength of the resonances is determined by radiative damping. For orbital periods on the order of ~ 4 days, γ can become comparable to γ' . Then the damping factor in 17 has to be replaced by $(\gamma + \gamma')^2$, and the strength of the resonance is reduced by a factor ~ 4 .

We first consider the effect on the circularization timescale of *varying the parameters c_1 , c_2 , s and Λ* in the expression (13) for ν . Note that the denominator we used in this expression is $1 + c_2(m t_c/P_o)^2$ rather than $1 + c_2(m \omega t_c)^2$. Using the latter with $c_2 = 1$ is equivalent to setting $c_2 = (2\pi)^2$ in the former. At present, it seems that our knowledge of convection does not allow discrimination between these possibilities (see, for example, the discussion in Zahn 1989). However, we note that Goodman & Oh (1997) have recently put forward some arguments in favor of $c_2 = (2\pi)^2$. Using $c_2 = (2\pi)^2$ in (13) results in a circularization time for $P_o = 12.4\text{ d}$ that is 10 times larger than that obtained with $c_2 = 1$. If we set $c_2 = 0$, t_{circ} is decreased by only a factor 2. This is because when $c_2 = 1$ the factor $c_2(m t_c/P_o)^2$ is already smaller than, or even very small compared to, unity in a large part of the convective envelope. Thus it seems that adjusting the way in which turbulent viscosity responds to short period forcing cannot produce the required enhancement in this case.

In Table 2 we summarize the results obtained for different values of s and c_2 , and in Table 3 we indicate the corresponding index of the power law in expression (37). We note that $c_2 = 1$ corresponds to the denominator in (13) being $1 + (m t_c/P_o)^s$, whereas $c_2 = (2\pi)^s$ corresponds to $1 + (m \omega t_c)^s$.

We note that setting $c_2 = (2\pi)^2$ with $s = 2$ decreases the index of the power law in (37) down to ~ 3.3 . This gives t_{circ} proportional to the orbital period to the $\sim 11/3$, which is similar to the

Table 2: t_{circ} for different values of s and c_2

P_o (days)	c_2	s	t_{circ} (Gyr)
4.23	1	2	2.46
–	–	1	1.37
12.4	–	2	220
–	–	1	211
4.23	$(2\pi)^2$	2	39.4
–	2π	1	5.98
12.4	$(2\pi)^2$	2	2010
–	2π	1	685

Table 3: Index of the power law in (37) for different values of s and c_2

c_2	s	Index of the power law
1	2	3.85
–	1	4.3
$(2\pi)^2$	2	3.3
2π	1	4.1

value found by Goldman & Mazeh (1991).

Zahn & Bouchet (1989) have argued that the prescription $s = 2$ suggested by Goldreich & Keeley (1977) and used later by Campbell & Papaloizou (1983) and Goldman & Mazeh (1991) (see also Goodman & Oh 1997) would lead to cutoff periods in clear conflict with the observational data which they claim require $s = 1$. The results presented for the model adopted here do not support this statement. If $c_2 = 1$, t_{circ} hardly changes when s is changed from 2 to 1. If $c_2 = (2\pi)^s$, the difference between $s = 1$ and $s = 2$ is not dramatic for $P_o \sim 8 - 12$ d. Within the uncertainties associated with convection, our results do not allow a distinction to be made between $s = 1$ and $s = 2$.

Finally, taking the mixing length to be the distance to the top boundary of the convective envelope rather than 3 times the pressure scale height does not affect significantly the circularization timescale.

We note that the torque is directly proportional to c_1 and α^2 . However, c_1 is expected to be on the order of unity, and α is usually taken to be between 1 and 4.

3.4.2. Modifications to the Brunt-Väisälä frequency

The magnitude of the turbulent viscosity given by (13) would be increased if the magnitude of the Brunt-Väisälä frequency was larger in the convection zone. This is because the convective timescale decreases. We comment that a reduction in the convective timescale, while maintaining the same length scale, implies larger convective velocities which would have to occur without increasing the heat flux. This is the essential feature of the modification. To illustrate the effect of increasing the Brunt-Väisälä frequency we consider the following dimensionless number:

$$\eta = \frac{N^2}{g} \left(\frac{d \ln P}{dr} \right)^{-1},$$

which is the superadiabatic temperature gradient when radiation pressure and variations of the mean molecular weight are neglected. The accuracy with which η is known from helioseismic observations is not better than $\sim 10^{-2}$ (Gough 1984). However, in most of the convective envelope, this parameter, estimated from mixing length theory applied to a non-rotating stars, is much smaller than 10^{-2} .

We have made a numerical investigation in which we increased $|N^2|$ in the convection zone by replacing η by $\min(p\eta, 10^{-3})$, p being an arbitrary constant, wherever $\eta \leq 10^{-3}$ (except just below the outer radius of the convective envelope). We have considered $p = 50$ and $p = 100$. It is doubtful that consideration of present helioseismic data could preclude such an increase of $|N^2|$ (Thompson 1997).

Figure 5 shows η in the convective envelope versus x for the original solar model and for $p = 50$ and $p = 100$. We also display the factor by which $|N^2|$ has been increased in each case.

The circularization timescales we find with $c_2 = 1$ and $s = 2$ for $P_o = 12.4$ d when $p = 50$ and $p = 100$ are respectively 13 and 7.7 Gyr , which are now larger than the observed value by factors of 3 and 2 respectively. Small discrepancies of this magnitude could be dealt with by adjustments to the mixing length or c_1 . When either $p = 50$ or $p = 100$, the circular orbit torque is found to be proportional to $\omega^{4.6}$.

If, keeping $s = 2$, we adopt $c_2 = (2\pi)^2$, t_{circ} is increased only by a factor 1.3 compared to the case $c_2 = 1$ for $p = 100$. This is because the factor $c_2(m t_c / P_o)^2$ is smaller than, or even very small compared to, unity in almost all the convection zone whatever c_2 between 1 and $(2\pi)^2$.

Although an increase in $|N^2|$ of the magnitude we consider might be thought to be unrealistic, we note that such an increase in the deep layers of the convection zone has also been considered by D'Silva (1995) as a means of explaining the dynamics of sunspots without invoking too strong a magnetic field. In his model, which applies strictly to a star rotating at the same rate as the sun, $|N^2|$ has to be larger than $4 \times 10^{-11} s^{-2}$, which means that it has to be multiplied on average by a factor ~ 8 . In the solar model we use, we need to multiply $|N^2|$ by a factor between 100 and 400 for $0.722 \geq x \geq 0.713$, between 10 and 100 for $0.828 \geq x \geq 0.722$ and between 1 and 10

for $0.915 \geq x \geq 0.828$ in order to get such a minimum value. If we do this, the circularization timescale we get for $P_o = 12.4$ d is only 6 times larger than the observed one. In this context, it is possible that if the proposed increase in $|N^2|$ is related to the stellar rotation, this may be even greater for the more rapidly synchronously rotating star that is expected in the equal mass binary case.

We note that numerical simulations of turbulent convection in the presence of rotation show an increase of $|N^2|$ with the effect of rotation (Brummell, Hurlburt & Toomre 1996). This is because, as pointed out by Brummel *et al.* (1996), rotation influences the thermodynamic mixing properties of the convection in such a way that it leads to a decrease in correlation between temperature fluctuations and vertical velocities. The efficiency of the vertical convective transport is then weakened, with a subsequent enhanced superadiabatic mean stratification in the interior of the fluid (see their Figure 8.a).

This suggests that the magnitude of the Brunt-Väisälä frequency in the convective envelope of rotating stars is actually larger than the values given by the solar model we have been using here. However, it seems questionable that the extremely large increase required to account for the observed circularization rates can be achieved.

3.4.3. Turbulent Viscosity below the convection zone

Another means of increasing the total amount of dissipation is to assume that turbulent viscosity acts down to some depth below the inner boundary of the convective envelope. This might be expected if convective overshooting takes place. However, this might not be a very effective process because of the slow convective motions expected and the rapid increase in $|N^2|$ that occurs as the radiative zone is entered.

Estimates based on the observed solar oscillation frequencies give an upper limit between 0.05 (Basu 1997) and ~ 0.1 (Christensen-Dalsgaard, Monteiro & Thompson 1995) times the pressure scale height on the extent of overshoot below the convection zone.

Here we consider a simple illustrative situation in which convective blobs or some other turbulent motions are able to penetrate into the stratified radiative core over some fraction z of the pressure scale height $|d\ln P/dr|^{-1}$ producing a turbulent viscosity. We model this by setting ν to be constant from a distance $0.5z|d\ln P/dr|^{-1}$ above the inner radius of the convective envelope down to the same distance below this radius, equal to its value at the top of this zone. Because such a viscosity is able to act on the short wavelength part of the tidal response associated with g modes it has a dramatic effect.

For $z = 1$ and $c_1 = c_2 = 1$, the circularization timescale for $P_o = 12.4$ d is decreased by a factor about 400, being now 8 times smaller than the observed timescale. If we set $c_2 = (2\pi)^2$ (see discussion above), t_{circ} is increased by a factor 15, being about 4 times larger than the observed timescale.

For $z = 0.1$ and $c_1 = c_2 = 1$, we get a circularization timescale for $P_o = 12.4$ d about 30 times larger than the observed one. For the calculated timescale to be in agreement with the observations, we need z between 0.4 and 0.5 with $c_1 = c_2 = 1$. In the model we have adopted, the effect is of less importance for shorter periods because the number of oscillations of the response in the region of the radiative core where turbulent dissipation is introduced decreases with forcing frequency. Therefore, the torque does not vary with ω as a simple power law with an index close to 4. However, in reality, the effectiveness of the turbulent viscosity should be reduced for short wavelength disturbances giving a compensating effect to make it relatively less effective at low frequencies.

The above calculations show that overshooting is not likely to be efficient enough to decrease the circularization timescales by a factor of about 50. To get such an effect, we indeed require an extent of overshoot below the convection zone at least 5 or 10 times larger than that deduced from the observations. In addition, we have not taken into account the fact that overshooting leads to an increase of the g modes length scale through a decrease in the buoyancy or the magnitude of N^2 . This in turn would decrease the amount of turbulent dissipation associated with overshooting.

3.5. Fitting the observations

As we have already mentioned above, *calculations based on both the dynamical and equilibrium tide theories give a torque proportional to the orbital frequency raised to a power ~ 4* (see 36 and 37). If circularization of solar-type binaries does occur through the action of turbulent viscosity on the tides, then its magnitude has to be calibrated so as to account for the observed timescale. We have discussed in the previous section, somewhat speculatively, how the required enhancement of the magnitude of the viscosity above that obtained from simple estimates might be envisaged to occur. Since the enhancement might depend on forcing frequency, it is not clear that the resulting torque will still be proportional to the frequency to the ~ 4 . However, the increase to $|N^2|$ described above gave torques that approximately preserved this power law so that in the absence of additional information, we shall suppose it holds. Then the calibration acts only to adjust the coefficient of the power law.

We note that the observations do not rule out any exponent between 3 and 5 (see below). Since our calculations can only strictly be applied to solar-type stars, we calibrate our results using $t_{circ} = 4$ *Gyr* for $P_o = 12.4$ d . This gives (in cgs):

$$\mathcal{T} \left(g \cdot cm^2/s^2 \right) = 5.086 \times 10^{35} \left(\frac{M_p}{M_p + M_\odot} \right)^2 \left(\frac{\omega}{10^{-5} s^{-1}} \right)^4, \quad (39)$$

or, equivalently:

$$\mathcal{T} \left(g.cm^2/s^2 \right) = 1.423 \times 10^{39} \left(\frac{M_p}{M_p + M_\odot} \right)^2 \left(\frac{P_o}{1 d} \right)^{-4}. \quad (40)$$

The corresponding formulæ for the orbital and spin up timescales (in giga–years) are:

$$t_{orb} (Gyr) = 2.763 \times 10^{-4} \frac{(M_p/M_\odot + 1)^{5/3}}{M_p/M_\odot} \left(\frac{P_o}{1 d} \right)^{13/3}, \quad (41)$$

$$t_{sp} (Gyr) = 1.725 \times 10^{-6} \left(\frac{M_p + M_\odot}{M_p} \right)^2 \left(\frac{P_o}{1 d} \right)^3, \quad (42)$$

and $t_{sp,c} = I_c t_{sp} / I$ (for the solar model we use, $I = 1.064 \times 10^{54} g.cm^2$ and $I_c = 1.5 \times 10^{53} g.cm^2$).

Since the torque is proportional to ω^4 , we can use the relation (35) for t_{circ} , so that the circularization time is given by

$$t_{circ} (Gyr) = 4.605 \times 10^{-5} \frac{(M_p/M_\odot + 1)^{2/3}}{M_p/M_\odot} \left(\frac{P_o}{1 d} \right)^{13/3}. \quad (43)$$

Even though our calculations can only be applied to solar–type stars, it is of interest to compare the circularization timescales we get from (43) with the observed ones. For $P_o = 4.3, 7.05, 8.5$ and $18.7 d$, (43) gives respectively $t_{circ} = 0.04, 0.3, 0.8$ and $24 Gyr$, to be compared with the observed timescales $0.003, 0.1, 0.8$ and $16 Gyr$ respectively. The agreement for $P_o \geq 8.5 d$ is within a factor 1.5. For smaller periods, circularization is expected to occur when the convective envelopes of the stars are larger, making turbulent dissipation more efficient. We note that Mathieu *et al.* (1992) have already pointed out that a power law $t_{circ} \propto P_o^{13/3}$ provides a close fit to the slope of the observed cutoff periods. However, the observations are equally well fitted with an index of $10/3$ and an index of $16/3$ cannot be ruled out (Mathieu *et al.* 1992).

If the simple estimate of the turbulent viscosity based on mixing length theory for non–rotating stars is used, the coefficients in the formulæ for the torque have to be divided by a factor ~ 50 whereas those in the formulæ for the timescales have to be multiplied by the same factor.

In Figure 6, we have plotted t_{orb} in units $(M_p/M_\odot + 1)^{5/3} / (M_p/M_\odot)$ and t_{circ} in units $(M_p/M_\odot + 1)^{2/3} / (M_p/M_\odot)$ versus ω and P_o in a log–log representation.

4. Discussion

4.1. Application to 51 Pegasi

It is of interest to apply these results to the system 51 Pegasi, for which the orbital period (assuming the observed oscillations are due to a companion) is $P_o = 4.23$ d. If the companion is a Jupiter mass planet ($M_p = 10^{-3} M_\odot$), then the tidal orbital evolution timescale given by (41) is $t_{orb} \sim 140$ Gyr, the star spin up timescale (42) is $t_{sp} \sim 130$ Gyr and the spin up timescale of the convective envelope is $t_{sp,c} \sim 18$ Gyr. All of these timescales are long compared with the inferred age of 51 Pegasi (Edvardsson *et al.* 1993). If the companion is a low-mass star of $0.1 M_\odot$, as has been recently suggested, t_{orb} is 100 times smaller while t_{sp} and $t_{sp,c}$ are 10^4 times smaller. We then expect the primary star to be synchronized with the orbit, in which case exchange of angular momentum is no longer taking place. Synchronization is actually expected if the mass of the companion is larger than about 10 Jupiter masses. The orbital decay timescale is also smaller than the age of the system, but since $t_{sp} < t_{orb}$, tidal interaction stops before the companion has plunged into the central star.

If the simple estimate of the turbulent viscosity based on mixing length theory for non-rotating stars is used, all these timescales have to be multiplied by ~ 50 . In that case, synchronization is expected if the mass of the companion is larger than about 70 Jupiter masses.

The planetary companion interpretation has been questioned recently by the reported 4.23 d modulation in the line profile of 51 Pegasi (Gray 1997), and the possibility that this modulation may be due to g mode oscillations has been considered (Gray & Hatzes 1997).

We note that, according to our results, such a modulation could not be due to g mode oscillations tidally driven by a companion. For the oscillation to have a period of 4.23 d, the orbital period would have to be 8.46 d. The maximum perturbed radial velocity at the surface of the star induced by the companion would then be between 2×10^{-3} and 1 m/s for a perturbing mass between 10^{-3} and 1 solar mass. *These numbers do not depend on the magnitude of the turbulent viscosity assumed, and are not expected to be affected by the possibility of resonance.* These velocities are at least about 50 times smaller than the observed ones.

4.2. Summary

In this paper, we have studied the dynamical response of the star to the tidal perturbation of a companion. We have computed the torque due to dissipation in the convective envelope using first-order perturbation theory. In the vicinity of resonance, we have also calculated the torque due to non-adiabaticity in the radiative core using a WKB treatment. We have found that the torque at effective resonances is mainly determined by radiative damping. We have carried out an analysis based on the adiabatic equilibrium tide, and showed that agreement with the dynamical tide calculations can be rather poor. For the unmodified stellar model and the periods of interest of several days, the torque derived using the equilibrium tide is 4 to 6 times larger than that

corresponding to the dynamical tide.

We have found that the presence of fixed resonances do not affect the long term orbital evolution of the binary, so that the different timescales (orbital evolution, circularization and spin up) are mainly determined by the non-resonant interaction. Our calculations show that the viscosity that is required to provide the observed circularization rates of solar-type binaries is ~ 50 times larger than that simply estimated from mixing length theory for non-rotating stars.

We have explored some means by which this viscosity might be enhanced. We have found that it could become large enough if the magnitude of the Brunt-Väisälä frequency in the deep convective envelope were increased sufficiently. Such an increase is expected to be produced by the effect of rotation on convection, but it is questionable whether it can be of sufficient magnitude.

We note that *the strength of the resonances for orbital periods larger than ~ 8 days and the perturbed velocity at the surface of the star are insensitive to the magnitude of the turbulent viscosity assumed.* Only for periods ~ 4 days is the strength of the resonances decreased by a factor ~ 4 . The effective widths of the resonances affecting the tidal torques as well are reduced when the viscosity is increased.

We have applied our results to 51 Pegasi, and showed that the oscillations which have been observed at the surface of this star cannot be a tidally driven non-radial g mode. Also we have found that the stellar rotation and the orbital motion of this system are expected to be synchronized if the mass of the companion exceeds 0.1 solar mass.

We are grateful to M.J. Thompson for supplying us a solar model, and thank D.O. Gough, R.D. Mathieu and M.J. Thompson for helpful discussions. This work is supported by PPARC through grant GR/H/09454 and by NSF and NASA through grants AST 93-15578 and NAG 5-4277. C.T. and D.N.C.L. acknowledge support by the Center for Star Formation Studies at NASA/Ames Research Center and the University of California at Berkeley and Santa-Cruz.

REFERENCES

Basu, S. 1997, MNRAS, 288, 572

Brummell, N. H., Hurlburt, N. E., & Toomre, J. 1996, ApJ, 473, 494

Campbell, C. G., & Papaloizou, J. C. B. 1983, MNRAS, 204, 433

Christensen-Dalsgaard, J., & Berthomieu, G. 1991, in Solar Interior and Atmosphere, ed. A. N. Cox, W. C. Livingston, & M. S. Matthews (Tucson: University of Arizona Press), 401

Christensen-Dalsgaard, J., Monteiro, M. J. P. F. G., & Thompson, M. J. 1995, MNRAS, 276, 283

Christensen-Dalsgaard, J. *et al.*, 1996, Science, 272, 1286

Claret, A., & Cunha, N. C. S. 1997, A&A, 318, 187

Cowling, T. G. 1938, MNRAS, 98, 734

Cowling, T. G. 1941, MNRAS, 101, 367

Darwin, G. H. 1879, Phil. Trans. Roy. Soc., 170, 1

D'Silva, S. 1995, ApJ, 443, 444

Edvardsson, B., Anderson, J., Gustafsson, B., Lambert, D. L., Nissen, P. E., & Tomkin, J. 1993, A&A, 275, 101

Goldman, I., & Mazeh, T. 1991, ApJ, 376, 260

Goldreich, P., & Keeley, D. A. 1977, ApJ, 211, 934

Goldreich, P., & Nicholson, P. D. 1989, ApJ, 342, 1079

Goldstein, H. 1980, Classical Mechanics (Addison-Wesley), 2nd Edition, p. 267

Goodman, J., & Oh, S. P. 1997, ApJ, 486, 403

Gough, D. O. 1984, Mem. S.A.It., 55, 13

Gray, D. F. 1997, Nature, 385, 795

Gray, D. F., & Hatzes, A. P. 1997, ApJ, 490, 412

Kumar, P., & Goodman, J. 1996, ApJ, 466, 946

Marcy, G. W., Butler, R. P. 1995, IAU Circ. 6251

Marcy, G. W., Butler, R. P., Williams, E., Bildsten, L., Graham, J. R., Ghez, A. M., & Jernigan, J. G. 1997, ApJ, 481, 926

Mathieu, R. D. 1992, in Binaries as Tracers of Stellar Formation, ed. A. Duquennoy, & M. Mayor (Cambridge: Cambridge University Press), 155

Mathieu, R. D. 1994, *ARA&A*, 32, 465

Mathieu, R. D., Duquennoy, A., Latham, D. W., Mayor, M., Mazeh, T., & Mermilliod, J.-C. 1992, in Binaries as Tracers of Stellar Formation, ed. A. Duquennoy, & M. Mayor (Cambridge: Cambridge University Press), 278

Mathieu, R. D., & Mazeh, T. 1988, *ApJ*, 326, 256

Mayor, M., & Queloz, D. 1995, *Nature*, 378, 355

Mayor, M., & Mermilliod, J.-C. 1984, in IAU Symposium 105, Observational Tests of Stellar Evolution Theory, ed. A. Maeder, & A. Renzini (Dordrecht: Reidel), 411

Papaloizou, J. C. B., & Savonije, G. J. 1985, *MNRAS*, 213, 85

Papaloizou, J. C. B., & Savonije, G. J. 1997, *MNRAS*, *submitted*

Press, W. H., Flannery, B. P., Teukolsky, S. A., & Vetterling, W. T. 1986, Numerical Recipes: The Art of Scientific Computing (Cambridge University Press), 2nd Edition

Rasio, F. A., Tout, C. A., Lubow, S. H., & Livio, M. 1996, *ApJ*, 470, 1187

Rieutord, M., & Zahn, J. P. 1997, *ApJ*, 474, 760

Savonije, G. J., & Papaloizou, J. C. B. 1983, *MNRAS*, 203, 581

Savonije, G. J., & Papaloizou, J. C. B. 1984, *MNRAS*, 207, 685

Savonije, G. J., Papaloizou, J. C. B., & Alberts, F. 1995, *MNRAS*, 277, 471

Savonije, G. J., & Papaloizou, J. C. B. 1997, *MNRAS*, *submitted*

Tassoul, J.-L. 1988, *ApJ*, 324, L71

Tassoul, J.-L. 1995, *ApJ*, 444, 338

Tassoul, M., & Tassoul, J.-L. 1997, *ApJ*, 481, 363

Thompson, M. J. 1997, Private Communication

Unno, W., Osaki, Y., Ando, H., Saio, H., & Shibahashi, H. 1989, Nonradial Oscillations of Stars (University of Tokyo Press), 2nd Edition

Xiong, D. R., Cheng, Q. L., & Deng, L. 1997, *ApJS*, 108, 529

Zahn, J. P. 1966, *A&A*, 29, 489

Zahn, J. P. 1975, A&A, 41, 320

Zahn, J. P. 1977, A&A, 57, 383

Zahn, J. P. 1989, A&A, 220, 112

Zahn, J. P., & Bouchet, L. 1989, A&A, 223, 112

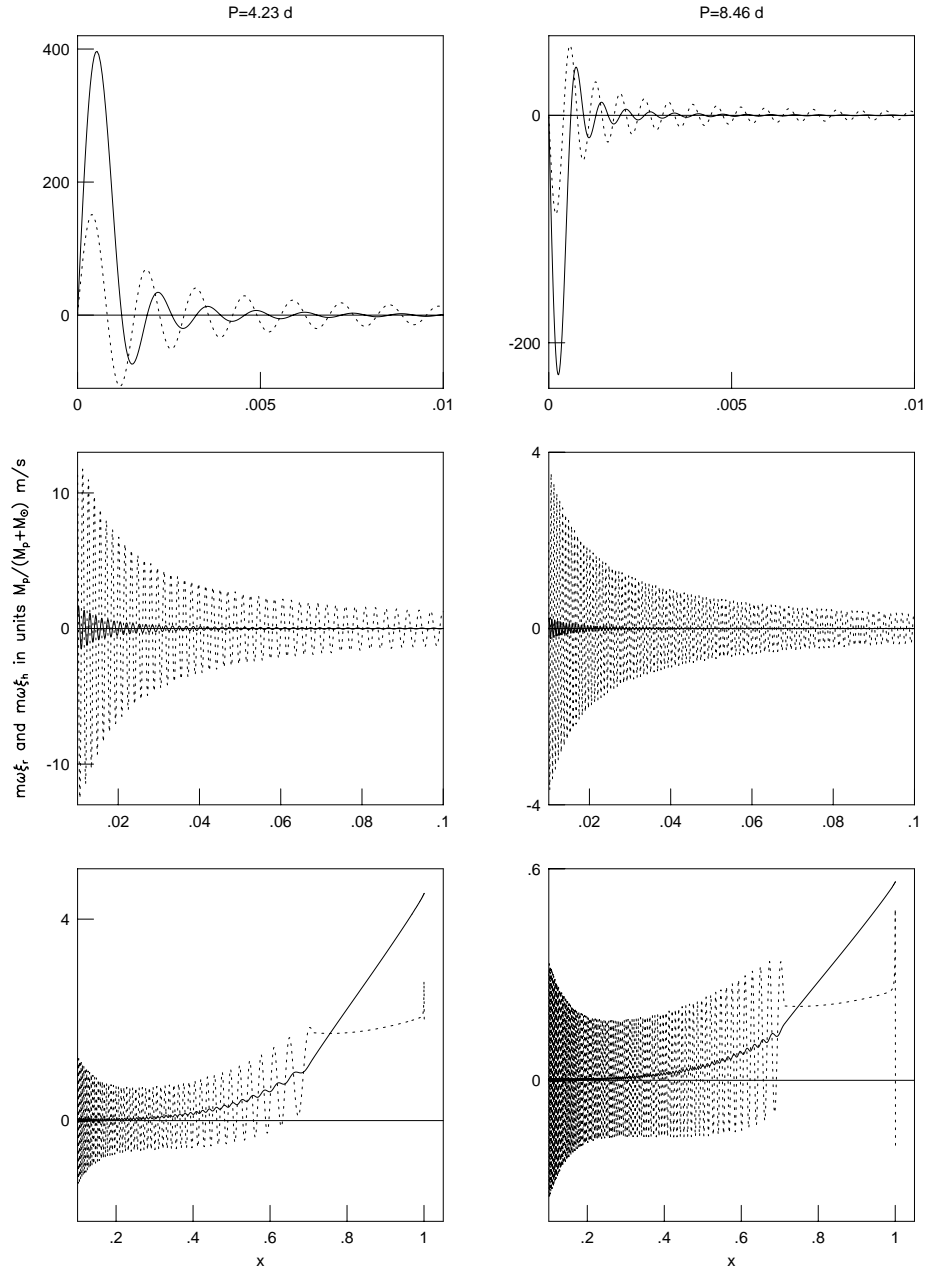


Fig. 1.— Real part of $m\omega\xi_r$ (solid lines) and $m\omega\xi_h$ (dotted lines) in units $M_p/(M_p + M_\odot) \text{ m/s}$ versus x for $x_{in} \leq x \leq 0.01$ (top panels), $0.01 \leq x \leq 0.1$ (middle panels) and $0.1 \leq x \leq x_{out}$ (bottom panels), and for $P_o = 4.23 \text{ d}$ (left panels) and $P_o = 8.46 \text{ d}$ (right panels). These represent typical values of the radial and horizontal velocities, the maximum values being three and six times larger respectively.

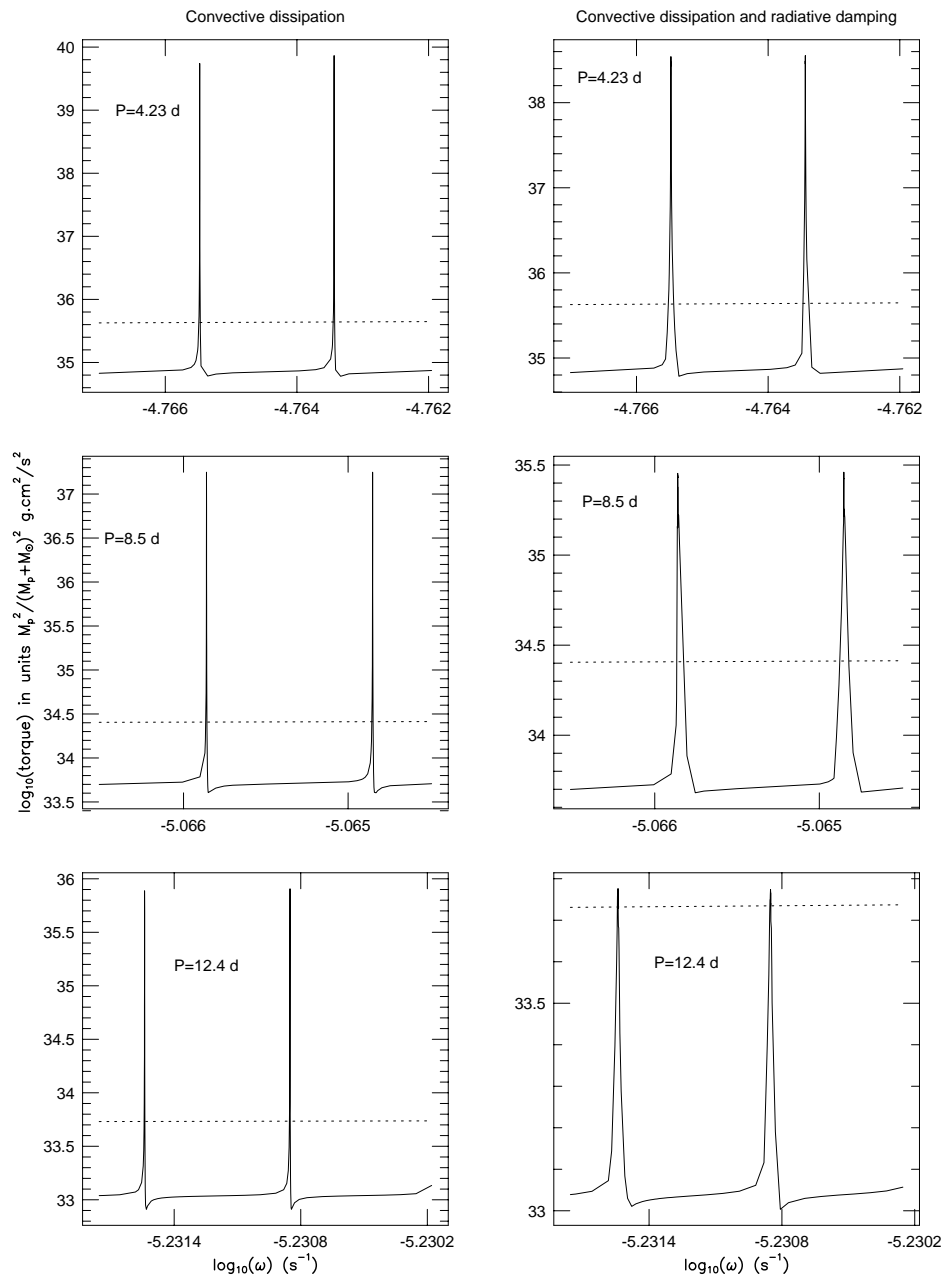


Fig. 2.— $\log_{10}(\mathcal{T})$ with \mathcal{T} in units $M_p^2 / (M_p + M_\odot)^2 \text{ g.cm}^2/\text{s}^2$ versus $\log_{10}(\omega)$ for $P_o = 4.23 \text{ d}$ (top panel), 8.5 d (middle panel) and 12.4 d (bottom panel). The solid and dotted lines correspond respectively to the dynamical and equilibrium tides calculations. On the left panels, \mathcal{T} is calculated using convective dissipation only. On the right panels, \mathcal{T} is calculated using radiative dissipation alone in the resonances and convective dissipation alone away from resonances.

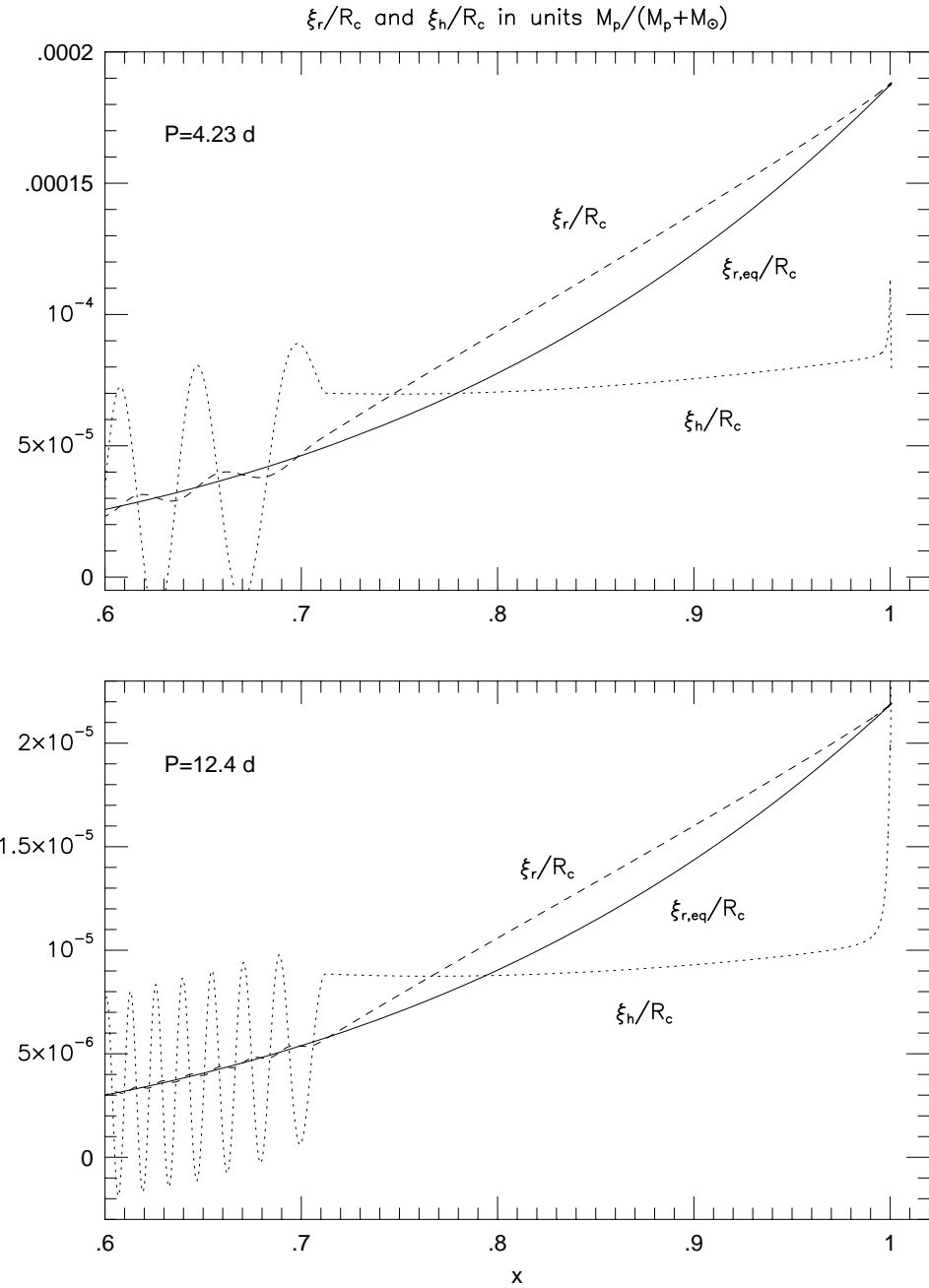


Fig. 3.— $\xi_{r,eq}/R_c$ (solid line), ξ_r/R_c (dashed line) and ξ_h/R_c (dotted line) in units $M_p/(M_p + M_\odot)$ versus x for $0.6 \leq x \leq x_{out}$, and for $P_o = 4.23$ d (top panel) and 12.4 d (bottom panel).

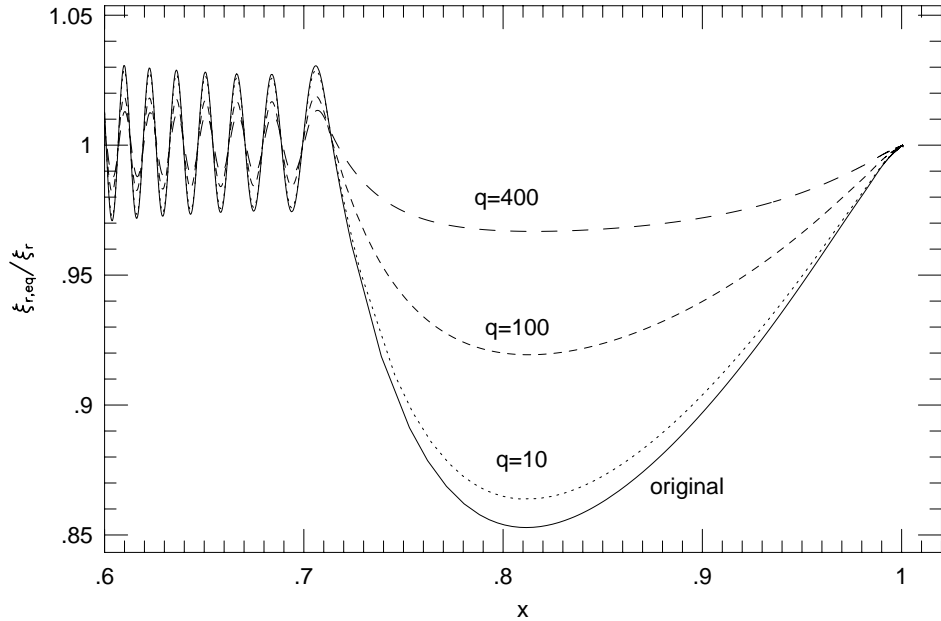


Fig. 4.— $\xi_{r,eq}/\xi_r$ versus x in the range $0.6 \leq x \leq x_{out}$ for $P_o = 12.4$ d and for $q = 10$ (dotted line), 100 (short-dashed line) and 400 (long-dashed line), the definition of which is given in the text. For comparison we have also plotted the case corresponding to the original solar model (solid line). $\xi_{r,eq}/\xi_r$ is close to 1 when $|N| \gg m\omega$.

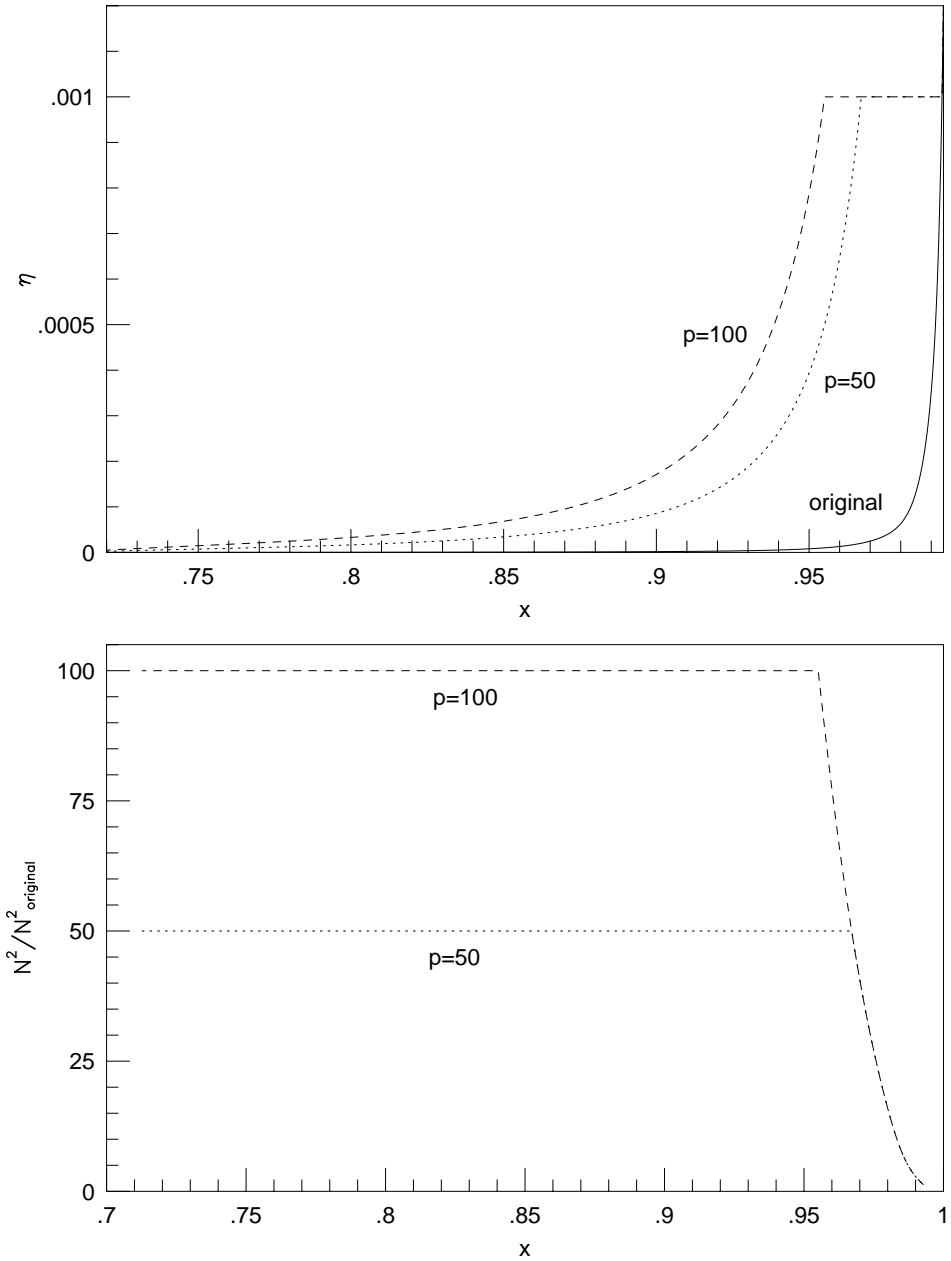


Fig. 5.— *Top panel:* Dimensionless parameter $\eta = N^2/(g d\ln P/dr)$ in the convective envelope versus x . The curves correspond to the original solar model (solid line), and to the models with increased $|N^2|$ ($p = 50$, dotted line, and $p = 100$, dashed line, where p is defined in the text). *Bottom panel:* Factor by which $|N^2|$ is increased in the convective envelope versus x . N^2_{original} corresponds to the original solar model, and N^2 corresponds to the models with $p = 50$ (dotted line) and $p = 100$ (dashed line).

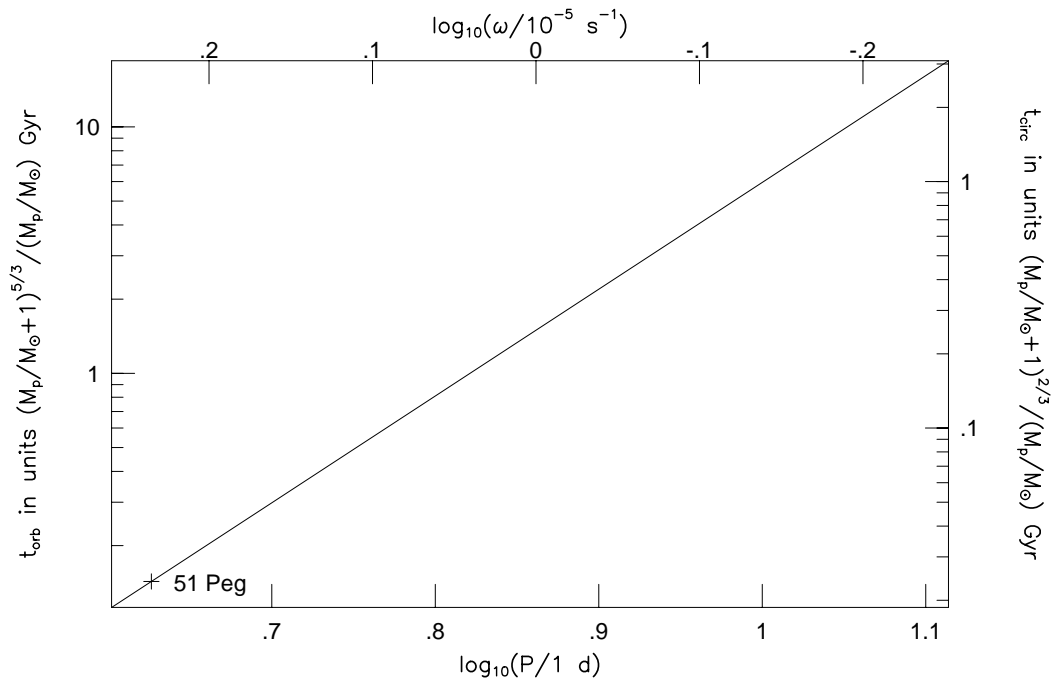


Fig. 6.— t_{orb} in units $(M_p/M_\odot + 1)^{5/3} / (M_p/M_\odot)$ Gyr (expression 41) and t_{circ} in units $(M_p/M_\odot + 1)^{2/3} / (M_p/M_\odot)$ Gyr (expression 43) versus ω and P in a log–log representation. The cross indicates the position of 51 Pegasi. These timescales fit the observations. *If instead they are calculated using the simple estimate of the turbulent viscosity based on mixing length theory, they have to be multiplied by ~ 50 .*